

Lake Baikal isotope records of Holocene Central Asian precipitation

George E. A. Swann^{1,*}, Anson W. Mackay², Elena Vologina³, Matthew D. Jones¹, Virginia N. Panizzo¹, Melanie J. Leng^{4,5}, Hilary J. Sloane⁴, Andrea M. Snelling¹, Michael Sturm⁶

¹*School of Geography, Centre for Environmental Geochemistry, University of Nottingham, University Park, Nottingham, NG7 2RD, UK*

²*Environmental Change Research Centre, Department of Geography, UCL, London, UK*

³*Institute of Earth's Crust, Siberian Branch of the Russian Academy of Sciences, Irkutsk, Russia*

⁴*NERC Isotope Geosciences Facilities, British Geological Survey, Nottingham, NG12 5GG, UK*

⁵*Centre for Environmental Geochemistry, School of Biosciences, Sutton Bonington Campus, University of Nottingham, Loughborough, LE12 5RD, UK.*

⁶*Eawag-ETH, Swiss Federal Institute of Aquatic Science and Technology, 8600, Dübendorf, Switzerland*

* *corresponding author george.swann@nottingham.ac.uk*

Keywords: Diatom; Mongolia; Paleoclimatology; Paleolimnology; Russia

Abstract

Climate models currently provide conflicting predictions of future climate change across Central Asia. With concern over the potential for a change in water availability to impact communities and ecosystems across the region, an understanding of historical trends in precipitation is required to aid model development and assess the vulnerability of the region to future changes in the hydroclimate. Here we present a record from Lake Baikal, located in the southern Siberian region of central Asia close to the Mongolian border, which demonstrates a relationship between the oxygen isotope composition of diatom silica ($\delta^{18}\text{O}_{\text{diatom}}$) and precipitation to the region over the 20th and 21st Century. From this, we suggest that annual rates of precipitation in recent times are at their lowest for the past 10,000 years and identify significant long-term variations in precipitation throughout the early to late Holocene interval. Based on comparisons to other regional records, these trends are suggested to reflect conditions across the wider Central Asian region around Lake Baikal and highlight the potential for further changes in precipitation with future climate change.

1 Introduction

The forest-steppe ecotone of Central Asia is dominated by grassland and taiga ecosystems that are vulnerable to both changes in the climate and other anthropogenic activities (Craine et al., 2012; Hijioaka et al., 2014; Settele et al., 2014; Tautenhahn et al., 2016). Declines in precipitation over the past three decades have led to marked reductions in grassland biomass across the Mongolian steppes and wider region (Endo et al., 2006; Liu et al., 2013; Li et al., 2015), whilst global reductions in boreal forest due to fire and forestry are second only to losses in tropical forests (Hansen et al., 2013). Ongoing work points to the continuing fragility of these ecosystems. For example, 21st Century climate change across Central Asia is likely to lead to a northward migration of the forest-steppe ecotone with remaining forest stand height highly dependent on rates of precipitation (Tchebakova et al., 2009; 2016). At the same time reductions in soil moisture associated with climate change are expected to accelerated grassland degradation, negatively impacting nomadic pastoralism (Liu et al., 2013; Sugita et al., 2015), whilst issues of water security are likely to be exacerbated by plans for increased groundwater extraction and dam construction (Karthé et al., 2015). Growth of hemi-boreal forests in the forest-steppe ecotone has already slowed, linked to decline soil water content due to regional warming (Wu et al. 2012).

Changes in the central Asian hydrological cycle will also alter regional carbon cycling. The increased risk of fires across grasslands and boreal forest will impact vegetation regeneration (Tchebakova, 2009; IPCC, 2012; Tautenhahn et al., 2016) and lead to an immediate increase in atmospheric CO₂ (Randerson et al., 2006). Reductions in soil moisture availability and rising temperatures will further reduce carbon terrestrial storage by increasing the decomposition of organic matter in soils and lowering net carbon uptake by plants (Lu et al., 2009; Crowther et al., 2016). However, more significant are the threats posed by permafrost degradation, particular in southern Siberia and northern Mongolia where permafrost is vulnerable to degradation through warming, human impacts and increased wildfires (Sharkuu, 1998; Romanovsky et al., 2010; Zhao et al., 2010; Törnqvist et al., 2014). Combined, these processes will release carbon to the atmosphere (Schuur et al., 2015) and increase organic carbon export to water bodies (Selvam et al., 2017).

In order to improve future predictions of the Central Asian hydrological cycle there is an urgent need to understand long-term changes in the climate system beyond the instrumental record. Here we use the oxygen isotope composition of diatom silica ($\delta^{18}\text{O}_{\text{diatom}}$) from Lake Baikal (Russia) to constrain historical changes in

Central Asian precipitation over the last 10,000 years, within the context of the modern day. Situated at the edge of the forest-steppe ecotone, the lake's catchment extends into northern Mongolia (Fig. 1) and is highly sensitive to changes in the hydrological cycle. Future changes in the region have the potential to reduce river flow around Lake Baikal, impacting the provision of water to one of the world's greatest lakes (Törnqvist et al., 2014) as well as decreasing soil moisture content and so increasing the risk of forest fires and associated carbon release (Forkel et al., 2012). Concurrently, climate change is likely to lead to further loss of permafrost across the region (Sharkuu, 1998; Törnqvist et al., 2014), potentially increasing the flow of dissolved organic carbon into Lake Baikal (Mackay et al., 2017) and altering the microbial food web, nutrient recycling and carbon processing within this ecological sensitive lake (Moore et al., 2009).

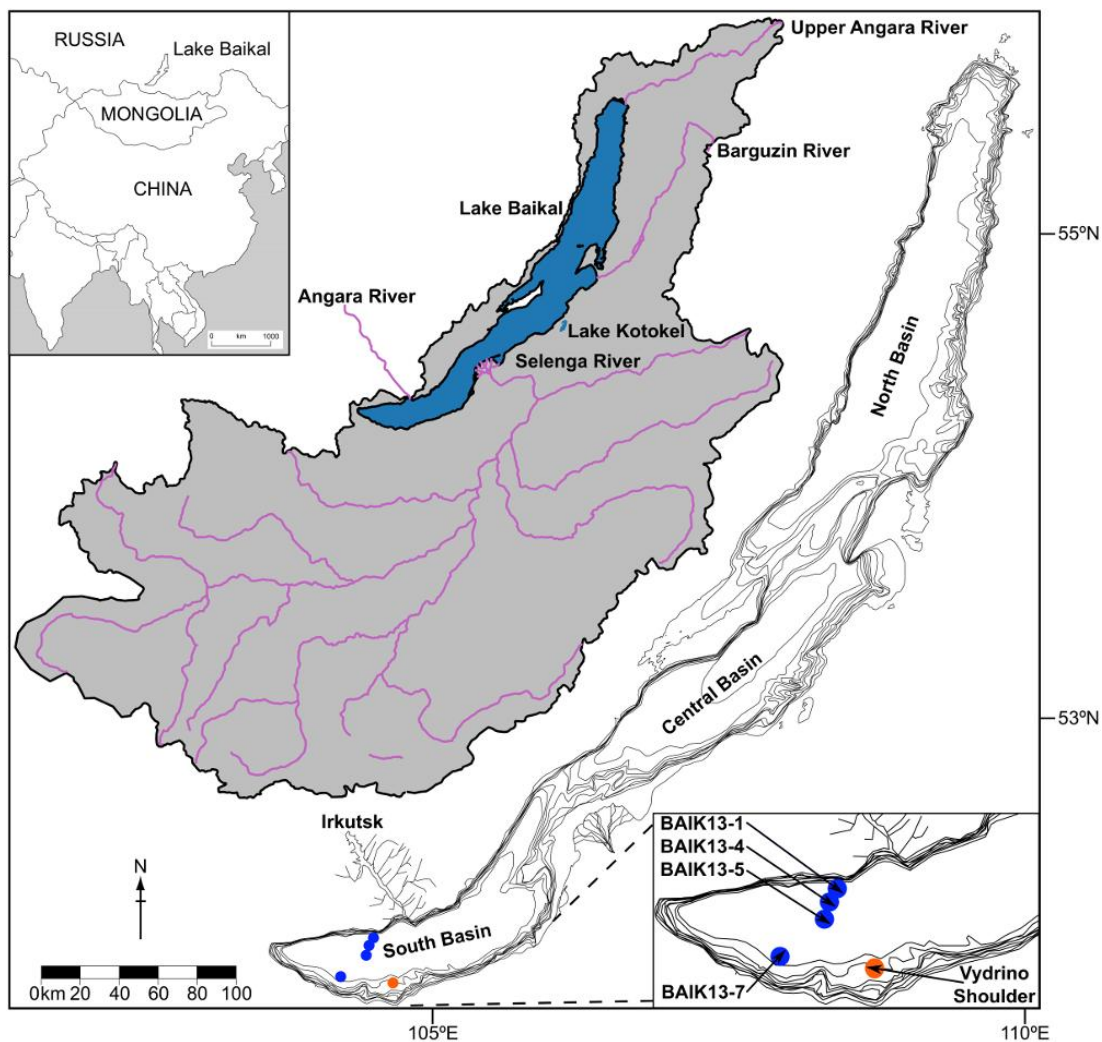


Figure 1: Location of Lake Baikal and its catchment (grey region) together with Lake Kotokel, the city of Irkutsk, major rivers, coring sites BAIK13-1, BAIK13-4, BAIK13-5, BAIK13-7 (blue circles) and Vydrino Shoulder (orange circle).

1.1 Lake Baikal reconstructions of the hydrological cycle

Lake Baikal is the world's oldest, deepest and most voluminous lake and, located in southern Siberia, contains c. 20% of the world's surface freshwater not stored within ice. The lake is divided into three basins (south, central and north) separated by the Buguldeika Saddle and the Academician Ridge, respectively (Fig. 1). Inputs of water to the lake are primarily derived from direct precipitation (c. 16%) and riverine inputs (c. 80%) (Seal and Shanks, 1998). Groundwater inputs are minor, believed to provide <4% of annual inflow (Seal and Shanks, 1998), although no systematic study has been carried out on groundwater, its residence time or isotope composition. Whilst over 350 rivers drain an area of c. 540,000 km² into Lake Baikal, inputs are dominated by the Selenga River, extending south into Mongolia, and the Upper Angara and Barguzin Rivers, draining the north of the catchment, which contribute c. 62%, 17% and 8% of riverine input respectively (Seal and Shanks, 1998) (Fig. 1).

Once in Lake Baikal, surface waters that extend down to the mesothermal maximum (MTM) at a depth of 200-300 m undergo convective mixing (Shimaraev et al., 1994; Shimaraev and Domysheva, 2004) and wind forced convection (Troitskaya et al., 2015). Whilst deeper waters are stratified (Shimaraev and Granin, 1991; Shimaraev et al., 1994; Ravens et al., 2000), they are exchanged across the MTM through periodic upwelling and downwelling episodes (Weiss et al., 1991; Shimaraev et al., 1993, 1994, 2012; Kipfer et al., 1996; Hohmann et al., 1997). Finally, water loss from Lake Baikal is dominated by outflow through the Angara River in the south basin of Lake Baikal (c. 79%) and evaporation (c. 19%), with an additional unconstrained loss from groundwater estimated at <2% of total outflow (Seal and Shanks, 1998; Shimaraev et al., 1994).

Over the past 15 years, significant effort has been devoted towards developing and applying $\delta^{18}\text{O}_{\text{diatom}}$ in palaeoenvironmental reconstructions due to its ability to reflect the isotope composition of ambient water ($\delta^{18}\text{O}_{\text{water}}$). With the controls on $\delta^{18}\text{O}_{\text{diatom}}$ similar to those for carbonates, $\delta^{18}\text{O}_{\text{diatom}}$ represents an important source of information in aquatic ecosystems such as Lake Baikal where carbonates are poorly preserved (Leng and Barker, 2006). In Lake Baikal, mixing of the water column leads to uniform surface and deep $\delta^{18}\text{O}_{\text{water}}$ of $-15.8 \pm 0.2\text{‰}$, whilst riverine inputs ($\delta^{18}\text{O}_{\text{river}}$) vary latitudinally from -13.4‰ to -21.2‰ in relation to the isotopically low winter precipitation in the north ($\delta^{18}\text{O}_{\text{p}}$) and higher summer $\delta^{18}\text{O}_{\text{p}}$ in the south (Seal and Shanks, 1998; Morley et al., 2005). With riverine inputs accounting for c. 80% of all inflow to the lake, spatial and temporal changes in $\delta^{18}\text{O}_{\text{p}}$ across the catchment have been proposed to change both $\delta^{18}\text{O}_{\text{river}}$ and the relative

balance of north versus south basin river discharge to the lake, processes that in turn alter $\delta^{18}\text{O}_{\text{water}}$ (Morley et al., 2005). On this basis, records of $\delta^{18}\text{O}_{\text{diatom}}$ can be used to monitor these changes in the regional Central Asian hydroclimate.

To date, this interpretation has been applied to interglacial records from Lake Baikal spanning the Holocene, MIS 5e and MIS 11 to constrain temporal variations in the penetration of westerlies into Central Asia and regional atmospheric circulation involving the Siberian High (Mackay et al., 2008, 2011, 2013). However, no empirical relationship has been demonstrated between hydroclimate variability and down-core records of $\delta^{18}\text{O}_{\text{diatom}}$. The absence of such a calibration prevents: 1) a full quantitative interpretation of the $\delta^{18}\text{O}_{\text{diatom}}$ data from Lake Baikal; 2) the integration of hydroclimate information in data-model comparisons to validate climate model outputs (e.g., Haywood et al., 2016; PAGES Hydro2k Consortium, 2017); and 3) insight of how the regional Central Asian climate behaved in intervals which might represent a future climate state. Here we consider point #1 through the presentation of new $\delta^{18}\text{O}_{\text{diatom}}$ data from a series of cores from the south basin of Lake Baikal that are compared to meteorological data over the last century and then employed to constrain historical changes in Central Asian precipitation through the Holocene. In demonstrating a relationship between $\delta^{18}\text{O}_{\text{diatom}}$ and precipitation, we highlight that levels of precipitation are today at their lowest levels for the last 10,000 years (10 ka), indicating the vulnerability of the region to future changes in precipitation and its associated impact on ecosystem disturbance and terrestrial carbon cycling.

2 Method

2.1 Sediment coring

Four short sediment cores were collected from the south basin of Lake Baikal in March and August 2013 using a UWITEC corer with PVC-liners (\varnothing 63 mm) which provided complete and undisturbed recovery of the highly susceptible sediment/water interface of the cores (Fig. 1). Multiple cores were collected from each of the sites in March 2013 through c. 78–90 cm of ice: BAIK13-1 ($51^{\circ}46'04.2''\text{N}$, $104^{\circ}24'58.6''\text{E}$, water depth = 1,360 m), BAIK13-4 ($51^{\circ}41'33.8''\text{N}$, $104^{\circ}18'00.1''\text{E}$, water depth = 1,360 m) and BAIK13-5 ($51^{\circ}39'01.9''\text{N}$, $104^{\circ}16'26.8''\text{E}$, water depth = 1,350 m). Further cores were then collected from BAIK13-7 ($51^{\circ}34'06''\text{N}$, $104^{\circ}31'43''\text{E}$, water depth = 1,080 m) in August 2013 aboard the Geolog research boat from the Institute of the Earth's Crust/Irkutsk (Fig. 1). At each site cores were labelled alphabetically with one core from each site (BAIK13-1C [50 cm], BAIK13-4F [33 cm], BAIK13-5C [42 cm], BAIK13-7A [47.5 cm]) sub-sampled in the

field at a resolution of 0.2 cm and transported to the UK for $\delta^{18}\text{O}_{\text{diatom}}$ analysis. Parallel cores (BAIK13-1A [49.3 cm], BAIK13-4C [38.3 cm], BAIK13-5A [43.4 cm], BAIK13-7B [47.2 cm]) were transferred to the Institute of the Earth's Crust/Irkutsk before being cut, photographed and lithologically described, based on smear slide inspection. A Bartington MS2E High Resolution Surface Scanning Sensor (Bartington, 1995) was used for non-destructive measurement of magnetic susceptibility (MS), with a resolution of 1 cm and reproducibility of <5%.

2.2 Age models

Dried samples from BAIK13-1C, BAIK13-4F and BAIK13-7A were analysed for ^{210}Pb , ^{137}Cs and ^{241}Am by direct gamma assay in the Environmental Radiometric Facility at University College London, using ORTEC HPGe GWL series well-type coaxial low background intrinsic germanium detector. No dating was carried out on core BAIK13-5C. Instead, results from BAIK13-5C are included for the purpose of qualitative comparisons with $\delta^{18}\text{O}_{\text{diatom}}$ data from other sites. ^{210}Pb was determined via its gamma emissions at 46.5 keV following storage for three weeks in sealed containers to allow radioactive equilibration. ^{137}Cs and ^{241}Am were measured by their emissions at 662 keV and 59.5 keV (Appleby et al, 1986). Corrections were made for the effect of self-absorption of low energy gamma rays within the sample (Appleby et al, 1992), with the absolute efficiencies of the detector determined using calibrated sources and sediment samples of known activity. To construct the final age-depth models a polynomial regression was fitted to the ^{210}Pb data with additional degrees added until no further improvements occurred in the fitted age-depth model against the old age-depth model under an ANOVA test at the 95% confidence interval.

2.3 Diatom oxygen isotopes

Thirty samples from cores BAIK13-1C, BAIK13-4F, BAIK13-5C, BAIK13-7A were prepared for diatom isotope analysis (see Supplementary Table 1) following the methodology in Swann et al. (2013) in which a combination of 5% HCl and 30% H_2O_2 are used alongside sodium polytungstate in heavy liquid separation at specific gravities of c. 2.2 g/ml^{-1} to remove non-diatom contaminants. Prior to analyses all samples were screened using a Zeiss Axiovert 40 C inverted microscope, scanning electron microscope (SEM) and X-ray fluorescence (XRF) to confirm sample purity and the absence of non-diatom contaminants. Diatoms in the analysed samples are dominated by mainly endemic species including *Aulacoseira baicalensis*, *Aulacoseira skvortzowii*, *Crateriportula inconspicua*, *Cyclotella minuta*, *Stephanodiscus meyerii* and *Synedra acus* var. *radians*. Given the functional ecology of taxa in the analysed samples, our isotope records are interpreted as

recording mean annual conditions with a small bias towards spring months when diatom productivity peaks shortly after ice break-up (Popovskaya, 2000). This is justified by the long residence time of water in the south basin (Shimaraev et al., 1994) and homogeneity in $\delta^{18}\text{O}_{\text{water}}$ across the modern lake (Seal and Shanks, 1998; Morley et al., 2005) which should lead to minimal intra-seasonal variations in both $\delta^{18}\text{O}_{\text{water}}$ and $\delta^{18}\text{O}_{\text{diatom}}$.

Samples were analyzed for $\delta^{18}\text{O}_{\text{diatom}}$ using a step-wise fluorination procedure at the NERC Isotope Geosciences Facility based at the British Geological Survey (Leng and Sloane, 2008). Isotope measurements were made on a Finnigan MAT 253 and converted to the Vienna Standard Mean Ocean Water (VSMOW) scale using the within-run laboratory diatom standard BFC_{mod} calibrated against NBS28. Where necessary, samples were corrected for oxygen bearing contaminants using a geochemical mass balance approach developed for Lake Baikal (Mackay et al., 2011). The issue of contaminants can be problematic in Lake Baikal due to aluminosilicates trapped within the cylindrical frustules of *Aulacoseira* species (Brewer et al., 2008). To account for this, contaminants were calculated using XRF Al_2O_3 concentrations following the mass-balance approach in Mackay et al. (2011) in which samples are corrected for an assumed diatom bound Al concentration of 0.3 wt%, and used to model contaminant oxygen using Lake Baikal end-members in which aluminosilicates contain 17.2% Al with a $\delta^{18}\text{O}$ composition of $11.7\text{‰} \pm 0.3\text{‰}$ (Brewer et al., 2008).

2.4 Climatological data

To assess the controls on $\delta^{18}\text{O}_{\text{diatom}}$, results were compared to climatological data from World Meteorological Organisation station 30710 (52°16'20" N, 104°18'29" E, elevation = 467 m), located in Irkutsk close to the south basin of Lake Baikal (Fig. 1) with data from 2016-1891 obtained via the KNMI Climate Explorer (<http://climexp.knmi.nl/>). For all statistical analyses, autocorrelation was checked for using a Durbin-Watson test. Unless specifically stated, datasets were not autocorrelated. Values of $\delta^{18}\text{O}_p$ were calculated following Seal and Shanks (1998) who established a relationship ($r^2 = 0.768$) between $\delta^{18}\text{O}_p$ and surface air temperature (SAT) of:

$$\delta^{18}\text{O}_p = 0.361 \cdot \text{SAT} - 16.798$$

(Eq. 1)

With >95% of water inputs to the lake originating from direct precipitation or riverine inputs (Seal and Shanks, 1998), changes in monthly isotopic inputs to Lake Baikal can be obtained by multiplying $\delta^{18}\text{O}_p$ by the amount

of monthly precipitation to account for seasonal variations in precipitation. Monthly values can then be summed to calculate annual inputs with values normalised relative to results for 2016 (δ_{influx}):

$$\delta_{\text{influx}} = \left(\frac{\sum_{\text{January}}^{\text{December}} \delta^{18}\text{O}_p \cdot \text{Precipitation (mm/month}^{-1})}{\text{Days in year}} \right) / \delta_{2016\text{influx}}$$

(Eq. 2)

3 Results

3.1 Core lithology

The deep water sediments of Lake Baikal are characterized by homogenous, fine-grained, and grey to olive-grey pelagic muds. They primarily consist of autochthonous biogenic material (mainly diatoms) with small amounts of allochthonous, terrigenous material (including pollen grains, clayey silts and a few sand grains). The entire water column of Lake Baikal is saturated throughout with oxygen, due to the regular renewal of the deep waters (Shimaraev et al., 1994; Tsimitri et al., 2015), which results in the oxidation of even the deepest surface sediment. Cores BAIK13-1A, BAIK13-4C, BAIK13-5A and BAIK13-7B are oxidized down to a depth of 2.0-3.6 cm, showing olive-brown, dark-brown to brownish-black colours (Fig. 2). Core BAIK13-7B recovered closer to the southern shore of the south basin consists of slightly more coarse-grained sediments with an increased content of silt and sand (Fig. 2). The homogenous pelagic muds of the deep-water basins of the lake are frequently intercalated by coarse turbidite layers. These graded beds are characterized by allochthonous, mostly terrigenous material, higher magnetic susceptibility and a graded texture, which grades upwards from a sandy base to silty-pelitic deposits with few sand admixtures and occasionally overlain at the top by a thin pelitic mud layer (Vologina et al., 2007; Sturm et al., 2016).

Several turbidites at different core depths and various thicknesses between 1.8 cm and 9.0 cm were observed in the cores, with two turbidites in BAIK13-1A, three in BAIK13-4C and six in BAIK13-5A (Fig. 2). The uppermost turbidites occur at 15.0–21.0 cm (BAIK13-1A), 2.0–5.3 cm (BAIK13-4C) and 3.5–9.0 cm (BAIK13-5A). There are layers of sand (21.8–22.5 cm) and sandy sediments (37.0–41.5 cm, 42.5–47.2 cm) without graded texture within sediment core BAIK13-7B. Lithological descriptions and MS-results were used to aid sampling of pelagic biogenic sediments (MS-values of up to 30×10^{-6} SI units) and avoid both turbidites and sandy layers (MS-values of up to 99×10^{-6} SI units).

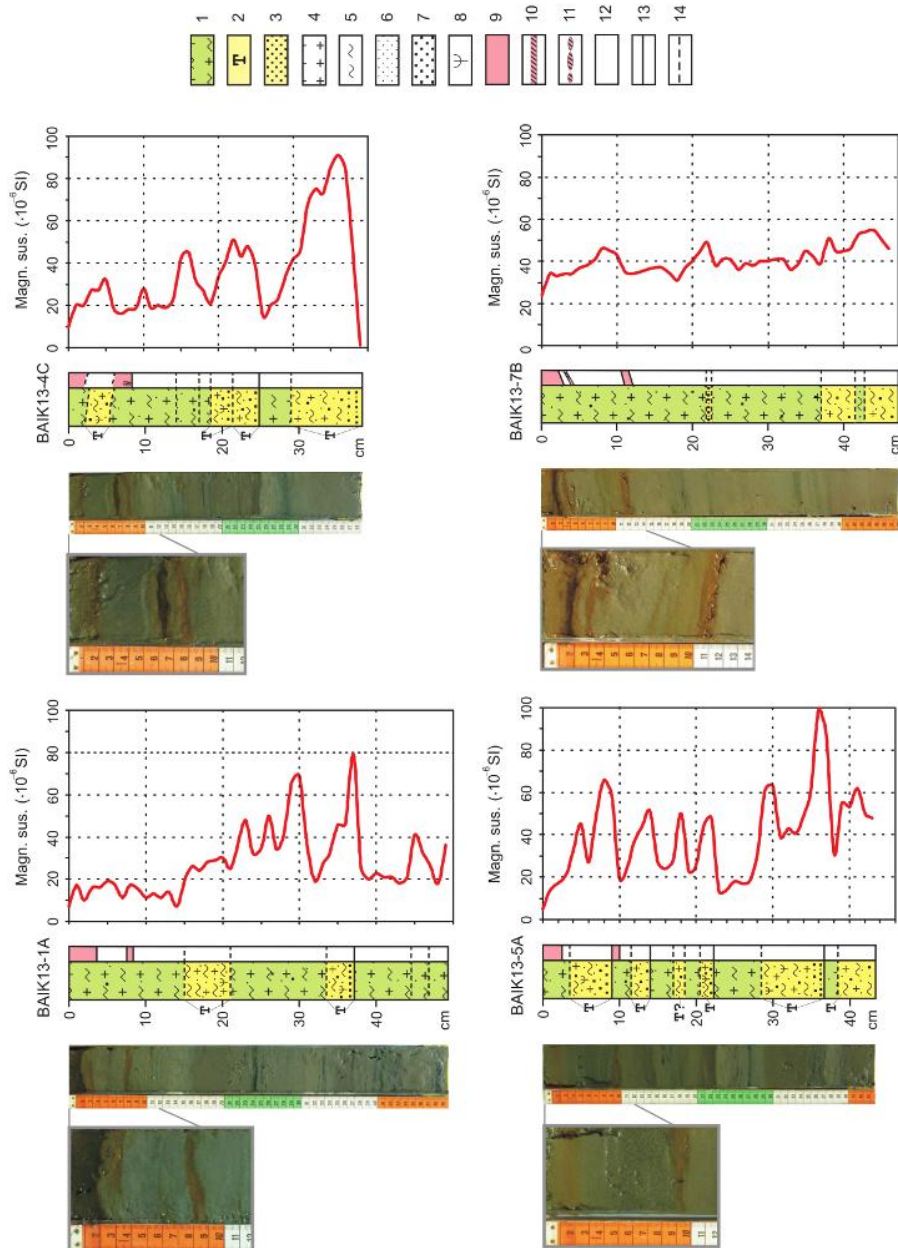


Figure 2: Photos, lithology and magnetic susceptibility of sediment cores BAIK13-1A, BAIK13-4C, BAIK13-5A and BAIK13-7B from the south basin of Lake Baikal. Lithology (left column): 1 - pelagic mud, 2 - turbidite, 3 - sandy sediment, 4 - diatoms, 5 - clay, 6 - silt, 7 - sand, 8 - land plant remains. Right column: 9 - oxidized sediment, 10 - Fe/Mn crust, 11 - fragments of Fe/Mn crust, 12 - O_2 reduced sediment. Boundaries between layers: 13 - distinct boundaries between layers, 14 - indistinct boundaries between layers.

3.2 ^{210}Pb age models

Total ^{210}Pb activity reaches equilibrium with supported ^{210}Pb at a depth of c. 5 cm (BAIK13-1C), 9 cm (BAIK13-4F) and 4 cm (BAIK13-7A). At sites BAIK13-1C and BAIK13-4F well resolved peaks of ^{137}Cs at 3.1 cm and 5.5-5.7 cm respectively likely relate to peak atmospheric testing of nuclear weapons 1963 AD. At all sites, non-monotonic variation in unsupported ^{210}Pb prevented the use of the constant initial concentration (CIC) dating model. Instead, ^{210}Pb dates were calculated using the constant rate of ^{210}Pb supply (CRS) model (Appleby and Oldfield, 1978). At BAIK13-1C and BAIK13-4F depths of 3.1 cm and 5.7 cm are dated to 1962/1963 AD respectively, both in agreement with the ^{137}Cs record. An absence of clear peaks in either ^{137}Cs or ^{241}Am at BAIK13-7A prevents validation of the ^{210}Pb dates. For all sites the final age-depth model shows a good fit to the ^{210}Pb dates (BAIK13-1C Adjusted $R^2 > 0.99$; BAIK13-4F Adjusted $R^2 = > 0.99$; BAIK13-7A Adjusted $R^2 > 0.99$) (Fig. 3). Mean uncertainty in the individual ^{210}Pb dates across all three cores is 6.8 years (BAIK13-1C: $\bar{x} = 7$, range = 2-26; BAIK13-4F: $\bar{x} = 8$, range = 2-30; BAIK13-7A: $\bar{x} = 3$, range = 2-6) (Fig. 3).

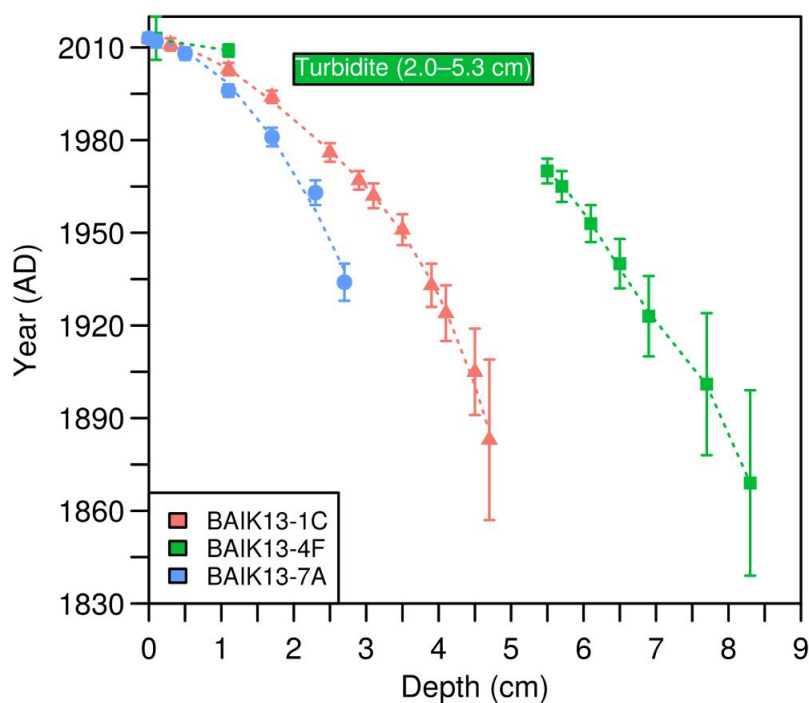


Figure 3: ^{210}Pb age-depth models for cores BAIK13-1C, BAIK13-4F and BAIK13-7A.

3.3 $\delta^{18}\text{O}_{\text{diatom}}$

Analysed samples from the four sediment cores cover the interval from c. 2010-1850 AD with raw $\delta^{18}\text{O}_{\text{diatom}}$ varying from +23.2‰ to +28.1‰ and replicate analyses of sample material indicating an analytical reproducibility (1σ) of 0.2‰ (Fig. 4a). Results from BAIK13-5C, which does not have an age model, display similar values and variations to those in BAIK13-4F and BAIK13-7C, although values at BAIK13-1C are

notably higher at +25.5‰ to +27.2‰. Levels of contamination were minimal for cores BAIK13-1C (\bar{x} = 0% contamination), BAIK13-4F (\bar{x} = 1.7% contamination) and BAIK13-5C (\bar{x} = 3.9% contamination) with Al/Si ratios of <0.02. At BAIK13-7C Si/Al ratios increase to 0.018-0.027 (\bar{x} = 0.023) indicating the need to account for aluminosilicates. Following correction for contaminants on samples at all sites, $\delta^{18}\text{O}_{\text{diatom}}$ ranges from +23.3‰ to +27.2‰ (\bar{x} = +24.5‰, 1σ = 1.0‰) (Fig. 4b) with the propagation of error associated with the correction increasing the analytical uncertainty for individual samples to 0.25-0.28‰. The two samples without XRF data are not considered further in this manuscript and all further mention of $\delta^{18}\text{O}_{\text{diatom}}$ refers to the corrected $\delta^{18}\text{O}_{\text{diatom}}$ dataset (Supplementary Table 1).

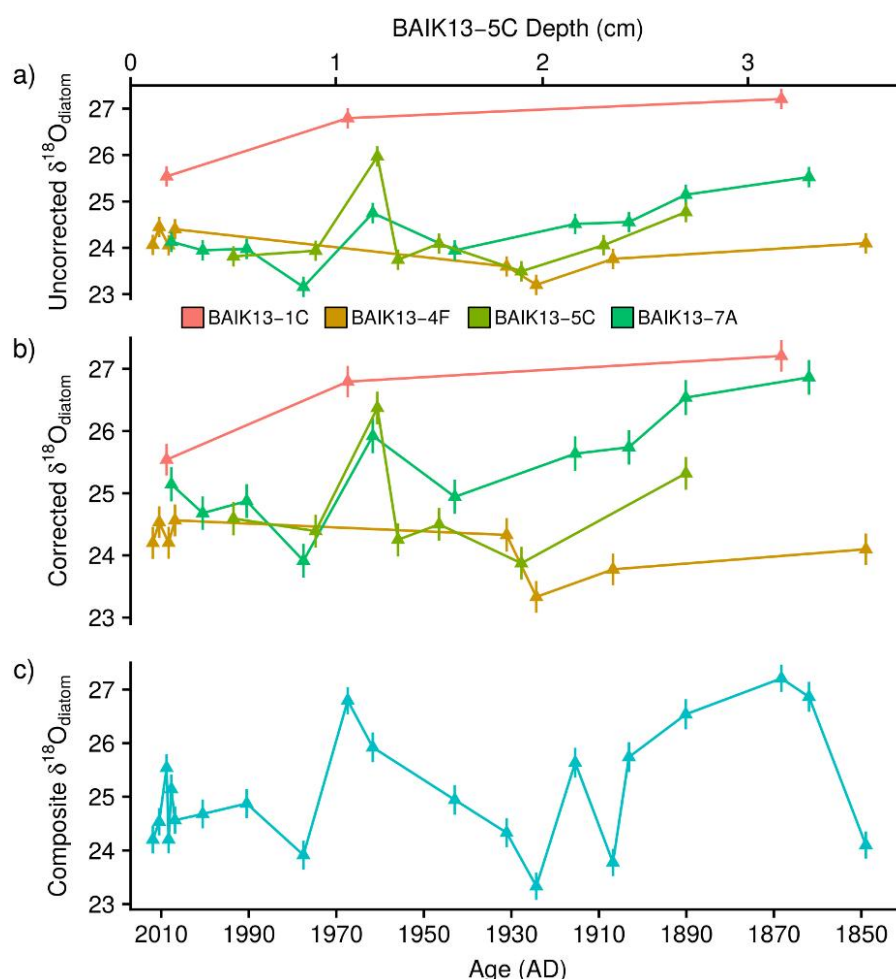


Figure 4: $\delta^{18}\text{O}_{\text{diatom}}$ from the south basin of Lake Baikal. Raw (uncorrected) (A) and corrected (B) $\delta^{18}\text{O}_{\text{diatom}}$ together with the composite south basin $\delta^{18}\text{O}_{\text{diatom}}$ record (C). All samples plotted against age except for BAIK13-5C, which are plotted against depth and not used in the final composite $\delta^{18}\text{O}_{\text{diatom}}$ record. Error bars for uncorrected $\delta^{18}\text{O}_{\text{diatom}}$ data are the 1σ analytical reproducibility (0.2‰) with error bars for the corrected $\delta^{18}\text{O}_{\text{diatom}}$ data reflecting the propagation of error associated with the correction for contaminants (range = 0.25-0.28‰).

On the basis of homogeneity in $\delta^{18}\text{O}_{\text{water}}$ across the modern lake and through the water column (Seal and

Shanks, 1998; Morley et al., 2005), $\delta^{18}\text{O}_{\text{diatom}}$ data from sites BAIK13-1C, BAIK13-4F and BAIK13-7C are combined to create a composite record of south basin $\delta^{18}\text{O}_{\text{diatom}}$ ranging from +23.3‰ to +27.2‰ (\bar{x} = +25.1‰, 1σ = 1.1) (Fig. 4c). After c. 1850 (+24.1‰), $\delta^{18}\text{O}_{\text{diatom}}$ increases in the second half of the 19th century to higher values of +25.1‰ to +27.2‰. Through the 20th century $\delta^{18}\text{O}_{\text{diatom}}$ is variable (\bar{x} = +24.2‰, 1σ = 1.1‰), particularly from 1960-1970 when $\delta^{18}\text{O}_{\text{diatom}}$ reaches a minimum of +23.2‰ by the end of the 1970's and a peak of +26.8‰ in the late 1960's. Values of $\delta^{18}\text{O}_{\text{diatom}}$ in the decade before the cores were collected in 2013 vary from +24.1‰ to +25.5‰ (\bar{x} = +24.5‰, 1σ = 0.6‰).

3.4 δ_{influx}

Mean annual precipitation in Irkutsk is 450 mm/yr with c. 75% of precipitation falling in the extended summer period from May to September, and only <10% falling in winter (DJF) (Fig. 5a). Surface air temperatures show similar seasonal variations from -20°C in January to +18°C in July (Fig. 5b). No systematic change in precipitation is apparent for recent decades, although precipitation from 2016-1926 (\bar{x} = 466 mm/yr) is notably higher than 1925-1891 (\bar{x} = 410 mm/yr, $p < 0.001$) after the step change in 1926 (Fig. 5c). In line with global records, SAT at Irkutsk show a prolonged warming trend over the monitoring record with marked increases from c. 1950 and c. 1990 onwards that are predominantly associated with increases in winter SAT (Fig. 5d). Annual and seasonal trends in precipitation and SAT from Irkutsk are similar to data from other sites around Lake Baikal, with similar trends observed in records of water inflow to the lake (Shimaraev et al., 2002; Frolova et al., 2017). As such, the meteorological data from Irkutsk can be regarded as being representative of the wider region.

Values of δ_{influx} shows mean inter-annual variations of c. 0.17 from 2016-1891 (Fig. 5e). On decadal timescales, from 1923-1891 δ_{influx} varies by c. 0.58 (\bar{x} = 0.79‰, 1σ = 0.13) before a long-term increase to the maxima in 1938 of 1.50, caused by exceptionally high June 1938 rainfall of 318 mm. Thereafter, values reveal a long-term decline from mean 1970-1950 values of c. 0.9 to mean values of 0.77 since the year 2000.

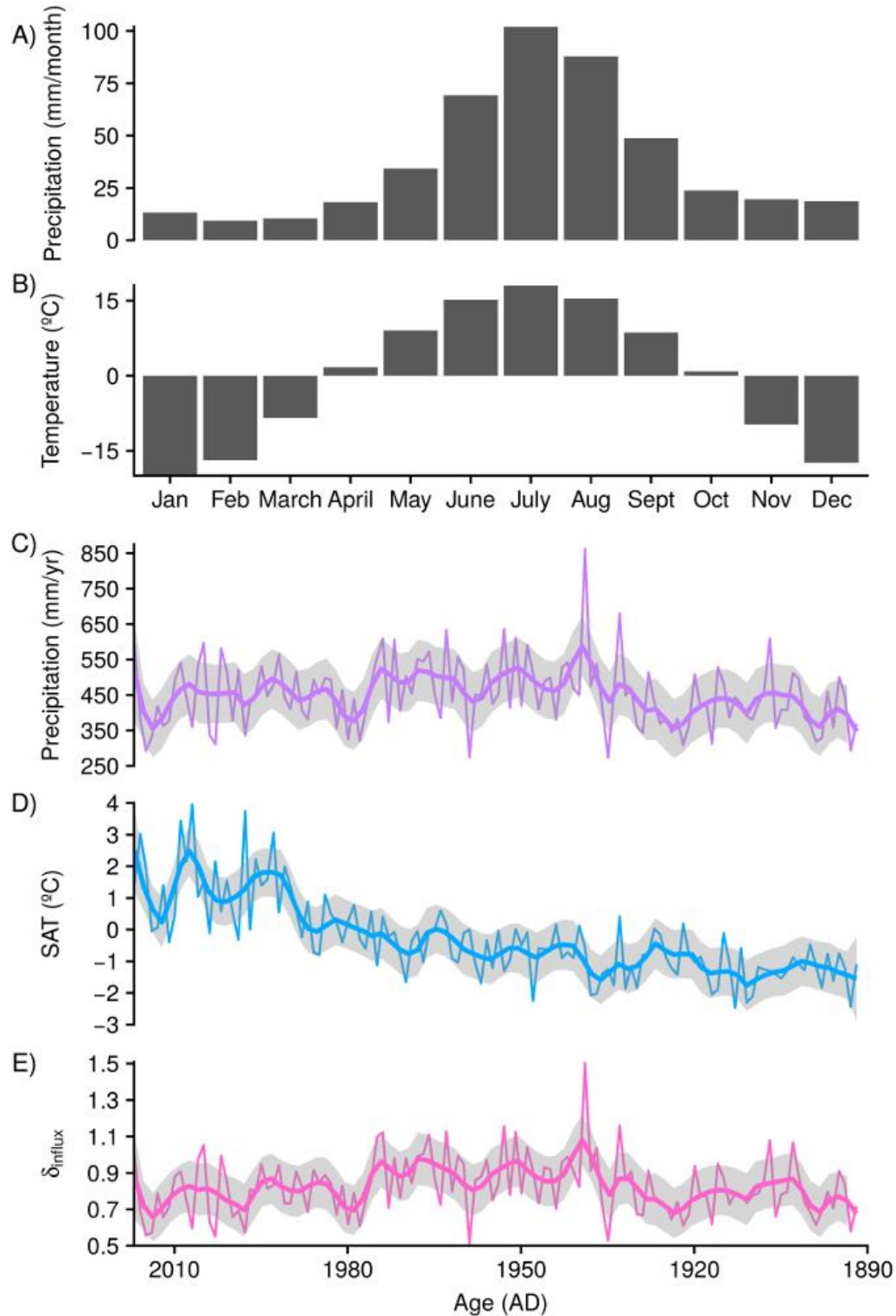


Figure 5: Meteorological data from Irkutsk (World Meteorological Organisation station 30710) showing the (A) monthly distribution of precipitation and (B) surface air temperature (SAT) alongside (C) temporal changes in precipitation and (D) surface air temperature from 2016-1891. Values of δ_{influx} (E) are calculated following Equations 1 and 2 with all values normalised relative to a value of 1 for 2016 AD. Thicker lines for panels C-E show locally weighted smoothing (loess) with shaded regions representing the 95% confidence interval on the fitted values.

3.5 Comparison of $\delta^{18}\text{O}_{\text{diatom}}$ and δ_{influx}

To account for uncertainty in the age-model and with analysed samples containing diatoms that accumulated over multiple years, a locally-weighted polynomial regression (lowess) was applied to δ_{influx} with a span of 10 years in order to enable robust comparisons with $\delta^{18}\text{O}_{\text{diatom}}$. From c. 2010-1900 change in $\delta^{18}\text{O}_{\text{diatom}}$ are significantly correlated to δ_{influx} ($r = 0.72$ $p = 0.001$) with a linear regression revealing a significant relationship between the two variables (Adjusted $R^2 = 0.48$, $p = 0.001$) (Fig. 6a). Whilst the residence time of water in the south basin is closer to 80-90 years (Shimaraev et al., 1994), the age of surface waters down to the mesothermal maximum (200–300 m water depth) are likely to be less, given reduced rates of mixing with deep/bottom waters (Weiss et al., 1991). The duration of vertical exchanges across the lake is limited to a short timeframe each year, with rates varying spatially across individual basins and between coastal and non-coastal sites (Weiss et al., 1991; Shimaraev et al., 1994; Ravens et al., 2000; Shimaraev et al., 2012; Troitskaya et al., 2015). With the mechanisms and extent of vertical mixing across Lake Baikal therefore remaining relatively unconstrained, it becomes impossible to accurately model the age of the ambient water in which the analysed diatoms photosynthesised. The span of 10 year employed in the regression of δ_{influx} is considered to be an appropriate estimate for this, given that surface $\delta^{18}\text{O}_{\text{water}}$ is likely to be significantly weighted towards more recent inputs to the lake.

Variance partitioning of δ_{influx} against surface air temperature and precipitation data from Irkutsk reveals 94% of the variability in δ_{influx} is related to changes in precipitation. This is confirmed by the strong relationship between δ_{influx} and annual precipitation at Irkutsk from 2016-1891 AD and hence between decadal smoothed annual precipitation (span = 10 years) and $\delta^{18}\text{O}_{\text{diatom}}$ (Adjusted $R^2 = 0.48$, $p = 0.001$, $\text{SE} = 26.9$ mm/yr) (Fig. 6 b,c). In contrast, there is no relationship between $\delta^{18}\text{O}_{\text{diatom}}$ and air temperatures at Irkutsk. From this relationship between $\delta^{18}\text{O}_{\text{diatom}}$ and precipitation, quantitative reconstructions of decadal averaged annual precipitation can be made from $\delta^{18}\text{O}_{\text{diatom}}$ with results, when applied to the south basin composite record, ranging from c. 400-520 mm/yr with variations between samples of up to 80 mm (Fig. 6d). These reconstructed estimates of precipitation are offset from actual measured levels of precipitation at Irkutsk by 5-45 mm/yr ($\bar{x} = 22.6$ mm/yr) (Fig. 6d).

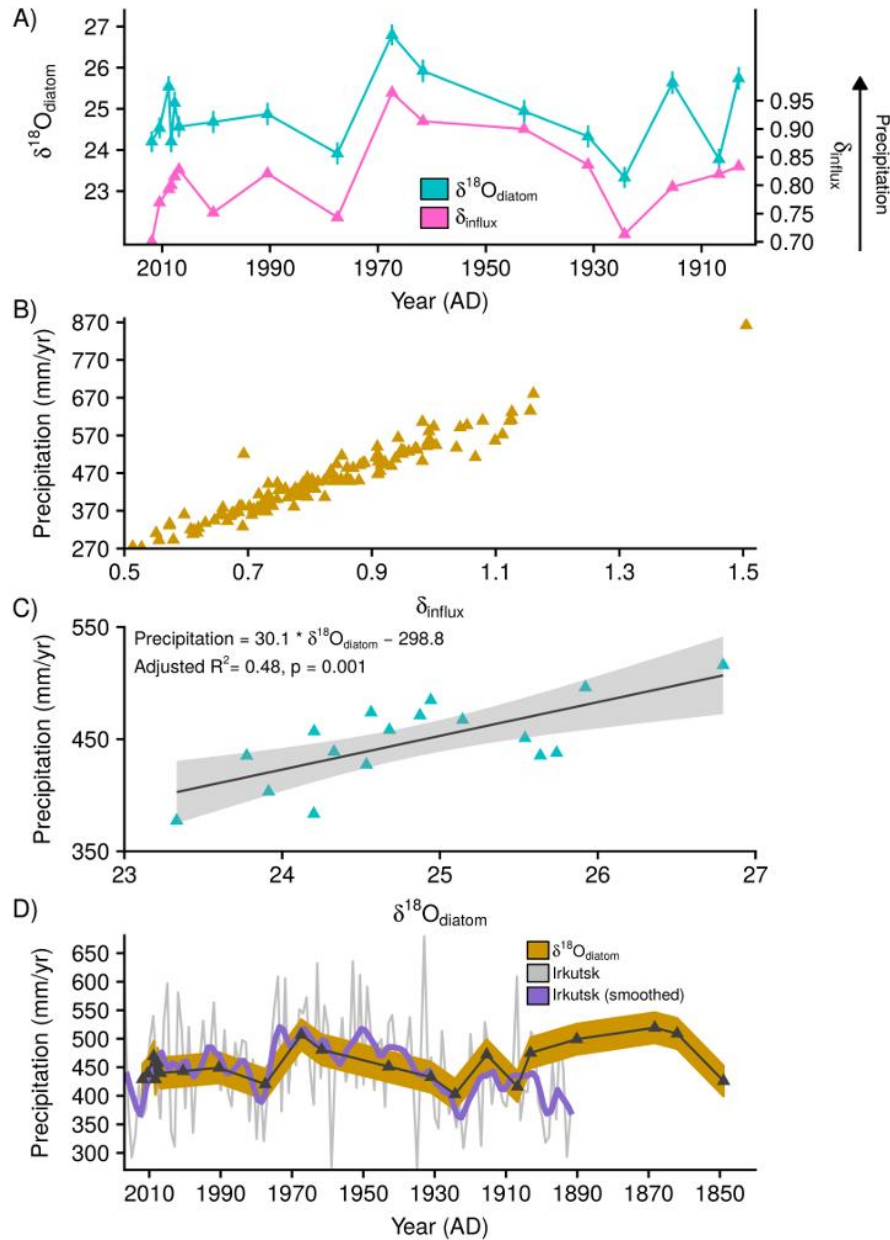


Figure 6: A) Composite $\delta^{18}\text{O}_{\text{diatom}}$ and δ_{influx} from c. 2010-1900 AD showing the strong correlation ($r = 0.72$ $p = 0.001$) and linear relationship (Adjusted $R^2 = 0.48$, $p = 0.001$) between the two variables. Displayed values of δ_{influx} are obtained from a locally weighted smoothing (span = 10 years) of the raw δ_{influx} data to account for uncertainty in the ^{210}Pb age model and accumulation of diatoms in the sediment record over multiple years. B) Relationship between raw δ_{influx} and Irkutsk annual precipitation from 2016-1891. C) Linear relationship between $\delta^{18}\text{O}_{\text{diatom}}$ and locally weighted Irkutsk precipitation (span = 10 years). D) Decadal annual precipitation reconstructed from $\delta^{18}\text{O}_{\text{diatom}}$ (brown region/black line) together with Irkutsk annual precipitation (grey) and locally weighted (span = 10 years) Irkutsk precipitation (purple). Shaded region for reconstructed precipitation is the standard error (26.9 mm/yr) of the regression model between $\delta^{18}\text{O}_{\text{diatom}}$ and Irkutsk precipitation (Fig. 6c). For clarity the y-axis has been scaled to not show the extreme Irkutsk precipitation of 861.9 mm $^{-1}$ in 1938 AD.

4 Discussion

4.1 $\delta^{18}\text{O}_{\text{diatom}}$ as an indicator of Central Asian precipitation

Both $\delta^{18}\text{O}_p$ and $\delta^{18}\text{O}_{\text{river}}$ in the Lake Baikal catchment fall on or close to the global meteoric water line (Seal and Shanks, 1998) with evaporation believed to not significantly impact $\delta^{18}\text{O}_{\text{water}}$ (Morley et al., 2005). With changes in the amount of precipitation dominating variations in δ_{influx} (Fig. 6b), δ_{influx} can be interpreted as primarily reflecting decadal changes in annual precipitation and in particular summer precipitation which accounts for 70-90% of annual precipitation to the region (Fig. 5b; Afanasjev, 1976; Shimaraev et al., 1994). As $\delta^{18}\text{O}_{\text{diatom}}$ reflects the isotope composition of ambient water in Lake Baikal, sedimentary records of $\delta^{18}\text{O}_{\text{diatom}}$ should also reflect changes in regional Central Asian precipitation across the wider region around Lake Baikal. This is supported by the strong correlation and relationship between δ_{influx} and $\delta^{18}\text{O}_{\text{diatom}}$, with increases (decrease) in $\delta^{18}\text{O}_{\text{diatom}}$ associated with higher (lower) δ_{influx} and an increase (decrease) in precipitation (Fig. 6a), as well as by the linear relationship between $\delta^{18}\text{O}_{\text{diatom}}$ and decadal smoothed annual precipitation (Fig. 6c).

Reanalysis data demonstrates that moisture transportation to the region throughout the year is primarily dominated by westerlies which, along with the Siberian High, control intra-annual variations in precipitation (Lydolph, 1977; Kurita et al., 2004), although we cannot rule out that other moisture sources may have become more dominant in the past beyond the observational record. In spring, the intensification of zonal circulation leads to the westerly progression of cyclones to the region, a process that intensifies in summer as low-pressure systems continue to develop along the Asiatic polar front (Lydolph, 1977; Chen et al., 1991; Shahgedanova 2002). With summer precipitation and inter-annual variations within it closely linked to eastward-propagating Rossby waves along the Asian Polar Front Jet (Iwao and Ttakahashi 2006, 2008), variations in summer Siberian precipitation have been linked to the Atlantic Multidecadal Oscillation (AMO) (Sun et al., 2015). Related to sea surface temperatures (SST) in the North Atlantic Ocean, the warm SST associated with a positive phase of the AMO are proposed to enhance precipitation across Siberia through a northerly shift in Rossby waves. Records of $\delta^{18}\text{O}_{\text{diatom}}$ from Lake Baikal can therefore now be employed to investigate long-term, decadal to centennial, controls on summer precipitation including the link between precipitation and the AMO. Debate exists over the extent to which the AMO will change in the future beyond natural fluctuations. Results from the IPCC AR5 report suggest that the AMO is unlikely to change its behaviour in a warmer climate state (Christensen et al., 2013). However, comparisons have shown the complexity in ensuring models adequately capture the characteristic of the AMO (Kavvada et al., 2013) whilst evidence exists for an amplification of the AMO at the

onset of industrial-era warming (Moore et al., 2017) and so the potential for further modifications with increased SST.

On the basis of our composite $\delta^{18}\text{O}_{\text{diatom}}$ record from the south basin of Lake Baikal and the link to δ_{influx} and $\delta^{18}\text{O}_p$ from 2011-1901 (Fig. 6a-c) we propose that $\delta^{18}\text{O}_{\text{diatom}}$ can be used to constrain annual precipitation and, given the seasonal distribution of precipitation, the summer position of the Asiatic polar front and associated jet system (Fig. 5b). This interpretation of $\delta^{18}\text{O}_{\text{diatom}}$ does not contradict previous records from Lake Baikal which related changes in $\delta^{18}\text{O}_{\text{diatom}}$ to the balance of north and south basin river inputs in Lake Baikal and so the wider hydroclimate of the region (Mackay et al., 2008, 2011, 2013). Instead, the relationship observed here now permits an enhanced understanding of the palaeoclimatology of the region by disentangling the dominant environmental controls on $\delta^{18}\text{O}_{\text{diatom}}$, precipitation and lake water temperature, allowing the quantification of past changes in Central Asia precipitation.

4.2 Holocene reconstruction of Central Asian precipitation

Precipitation data from Irkutsk is not available prior to 1891. Using the relationship between $\delta^{18}\text{O}_{\text{diatom}}$ and precipitation from c. 2010-1900 (Fig. 6c) we quantify decadal changes in annual precipitation for Central Asia from our composite south basin $\delta^{18}\text{O}_{\text{diatom}}$ record, which extends back to c. 1850 AD (Fig. 6d). Results show that the degree of variability in 21st and 20th century precipitation also prevailed through the late 19th century (426-519 mm/yr) with significantly lower levels of precipitation in c. 1850 relative to 1860-1890. Within the constraints of this low-resolution record and the regression standard error of 26.9 mm/yr, the results suggest that decadal annual precipitation in Central Asia has not notably changed in response to increased global/regional air temperature over the last c. 160 years (Fig. 6d). Observed reductions in Central Asian precipitation and river flow over recent decades (Liu et al., 2013; Li et al., 2015; Frolova et al., 2017) may therefore represent natural variability rather than an anthropogenic driven change.

Tree ring records from Mongolia currently provide regional hydroclimate data for the last 500 years (Pederson et al., 2001; Davi et al., 2006, 2009, 2010; Seim et al., 2017). However, longer precipitation records are needed, particularly over abrupt climate transitions and from geological analogues for the future to fully assess trends in Central Asian precipitation and possible links to the North Atlantic region. To place the results of the composite south basin core over the last c. 200 years within the context of natural variability, long-term changes in Central

Asian precipitation are reconstructed from a previously published corrected $\delta^{18}\text{O}_{\text{diatom}}$ record from Vydrino Shoulder (51.588N, 104.858E, Fig. 1) located off the southern shoreline of Lake Baikal (Mackay et al., 2011) using our $\delta^{18}\text{O}_{\text{diatom}}$ /precipitation calibration. The range of $\delta^{18}\text{O}_{\text{diatom}}$ in the core from Vydrino Shoulder (+25.3‰ to +31.1‰) (Fig. 7) is similar to that observed at nearby Lake Kotokel (+23.7‰ to +36‰), despite the significantly different controls and isotope setting of this smaller lake (Kostrova et al., 2013) (Fig. 1).

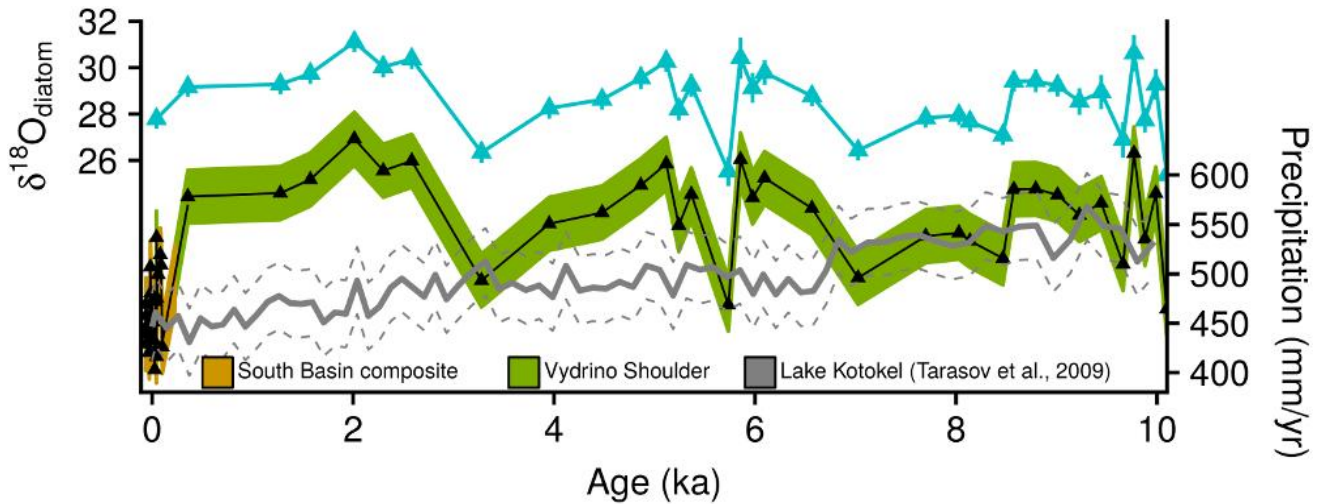


Figure 7: Holocene $\delta^{18}\text{O}_{\text{diatom}}$ from Vydrino Shoulder (51.588N, 104.858E, Fig. 1) located off the southern shoreline of Lake Baikal (Mackay et al., 2011) together with reconstructed precipitation at Vydrino Shoulder (green) and in the south basin composite record (brown) displayed in Figure 6d. One sample from the Vydrino Shoulder core (0.04 ka / 1907 AD) overlaps with the composite record in Figure 6. Shaded region shows range of reconstructed precipitation based on the standard error (26.9 mm/yr) of the regression model between $\delta^{18}\text{O}_{\text{diatom}}$ and Irkutsk precipitation (Fig. 6c). Also shown is the pollen inferred precipitation record from Lake Kotokel (solid grey line) (Tarasov et al., 2009) and the associated root mean square error of prediction (RMSE) of 34 mm/yr (Solovieva et al., 2005).

400

From 0-10 ka annual precipitation reconstructed from Vydrino Shoulder ranges from c. 470-640 mm/yr (\bar{x} = 565 mm/yr, 1σ = 40 mm/yr) (Fig. 7). No decline in precipitation occurs from c. 0.2-4.0 ka, but significant variability is apparent through the mid-Holocene warm interval from 5-9 ka (\bar{x} = 558 mm/yr, 1σ = 41 mm/yr). The record is notable in displaying values of precipitation that are markedly higher than those recorded at Irkutsk during the 20th and 21st Century, with values only comparable to mean modern day conditions (450 mm/yr) at 3.3 ka, 5.7 ka and 10.1-10.2 ka (Fig. 7). However, for 50% of the samples reconstructed $\delta^{18}\text{O}_{\text{diatom}}$ precipitation and their standard error fit with the range of Lake Kotokel pollen derived precipitation and their associated error (Tarasov et al., 2009) (Fig. 1, 7). This similarity between pollen and $\delta^{18}\text{O}_{\text{diatom}}$ precipitation is

most apparent in the early Holocene. In contrast, $\delta^{18}\text{O}_{\text{diatom}}$ precipitation is significantly higher than pollen precipitation for most of the mid/late Holocene interval.

4.2.1 Assessing the fidelity of the Holocene $\delta^{18}\text{O}_{\text{diatom}}$ record

It is necessary to consider possible issues that may have impacted the $\delta^{18}\text{O}_{\text{diatom}}$ record at Vydrino Shoulder given: 1) the mismatch between $\delta^{18}\text{O}_{\text{diatom}}$ and pollen derived precipitation during the mid/late Holocene; and 2) reconstructed $\delta^{18}\text{O}_{\text{diatom}}$ precipitation values from Vydrino Shoulder which are notably higher than those from the south basin composite record (Fig. 7). Diatom dissolution in Lake Baikal can be significant, with only 1% of diatoms preserved in the sediment record (Ryves et al., 2003; Battarbee et al., 2005). Of those preserved, dissolution indices indicate that 40-60% of all frustules over the last 1000 years show some form of dissolution (Mackay et al., 1998), increasing to 60-90% for MIS 5e (Rioual and Mackay, 2005). Despite this and the potential for samples from Vydrino Shoulder to have experienced higher rates of dissolution, work has conclusively shown that dissolution does not impact the silicon isotope signature in diatoms from Lake Baikal (Panizzo et al., 2016). In addition, laboratory experiments on a sample from Lake Baikal have shown that increased dissolution does not vary $\delta^{18}\text{O}_{\text{diatom}}$ beyond analytical error (Smith et al., 2016). Based on this, there is no evidence that the $\delta^{18}\text{O}_{\text{diatom}}$ signature in either the south basin composite record or the Vydrino Shoulder record is impacted by dissolution or other post-depositional processes.

The $\delta^{18}\text{O}_{\text{diatom}}$ reconstructed precipitation is also unlikely to be affected by Holocene changes in air temperature due to: 1) its negligible impact on δ_{influx} and $\delta^{18}\text{O}_{\text{diatom}}$ (Section 3.5); and 2) pollen derived reconstructions from both Lake Kotokel and the north basin of Lake Baikal that display “warmest month” temperature variations of only 2°C through the Holocene (Tarasov et al., 2007, 2009). The $\delta^{18}\text{O}_{\text{diatom}}$ /precipitation calibration assumes that both the moisture source region and the relative contribution of rivers flowing into Lake Baikal together with their seasonality has not significantly altered through the Holocene. Relative increase in winter precipitation/snow melt therefore has the potential to distort (lower) reconstructed precipitation due to the lower $\delta^{18}\text{O}_{\text{water}}$ that arises from colder atmospheric temperatures (Seal and Shanks, 1998). A similar effect may occur with significant increases in the relative inflow of more northerly rivers, such as the Upper Angara and Barguzin Rivers, given modern $\delta^{18}\text{O}_{\text{river}}$ compositions that are 4-6‰ lower than those for the Selenga River (Seal and Shanks, 1998). However, with summer precipitation accounting for 70-90% of annual precipitation (Fig. 5b; Afanasjev, 1976; Shimaraev et al., 1994) and with 62% of modern riverine inflow originating from the

Selenga River, it is difficult to envisage that Holocene hydrological conditions deviated sufficiently to alter $\delta^{18}\text{O}_{\text{diatom}}$ and the robustness of the $\delta^{18}\text{O}_{\text{diatom}}$ /precipitation calibration.

Based on the above and current knowledge on both $\delta^{18}\text{O}_{\text{water}}$ and $\delta^{18}\text{O}_{\text{diatom}}$ in Lake Baikal, it is not possible to attribute the mid/late Holocene offset between $\delta^{18}\text{O}_{\text{diatom}}$ and pollen precipitation reconstructions to methodological or proxy calibration issues. Instead, both the pollen and $\delta^{18}\text{O}_{\text{diatom}}$ reconstructions need to be considered as providing complementary information on precipitation trends across the catchment. When comparing the $\delta^{18}\text{O}_{\text{diatom}}$ precipitation reconstruction from Vydrino Shoulder to other records from the region, it is notable that results are broadly comparable to patterns of effective summer precipitation obtained from a low-resolution regional general circulation model (Bush, 2005). Pollen precipitation reconstructions from both Lake Baikal and Lake Kotokel display similar trends to one another through the Holocene (Tarasov et al., 2007, 2009) with the divergence away from $\delta^{18}\text{O}_{\text{diatom}}$ precipitation emerging after c. 7 ka, when pollen precipitation decreases by c. 10% with no corresponding change in $\delta^{18}\text{O}_{\text{diatom}}$ precipitation (Fig. 7). This decline in pollen precipitation around Lake Baikal also contrasts with records from the northern Mongolian Plateau (in the southern extent of the lake's catchment) which, similar to the $\delta^{18}\text{O}_{\text{diatom}}$ precipitation record from Vydrino Shoulder, show high rates of annual precipitation in both the early and late Holocene (Wang and Feng, 2013). Although records on the northern Mongolian plateau show a degree of spatial variability, no long-term decline in precipitation is apparent from c. 7 ka (Wang and Feng, 2013). Although it is beyond the remit of this study to evaluate the robustness of the pollen reconstructions, it is suggested that existing pollen records from Lake Baikal and Lake Kotokel (Tarasov et al., 2007, 2009) may reflect localised, site-specific, changes in precipitation. In contrast, given the size of Lake Baikal's catchment (540,000 km²) and with 83% of riverine inflow originating from the Selenga River and its tributaries, which extend into Mongolia, or the Upper Angara and Barguzin Rivers, which drain the region immediately to the east and north of Lake Baikal (Fig. 1), we propose that our $\delta^{18}\text{O}_{\text{diatom}}$ precipitation record from Lake Baikal reflects an amalgamated average of conditions across the wider Central Asian region incorporating the lake's catchment. If correct, this interpretation suggests that whilst pollen records indicate drier conditions immediately around Lake Baikal in the mid/late Holocene (Tarasov et al., 2007, 2009), the higher $\delta^{18}\text{O}_{\text{diatom}}$ records imply that long-term trends in precipitation elsewhere in the catchment and in particular to the south of the lake remained relatively constant between the early/late Holocene period, trends that are supported by individual records from northern Mongolian (Wang and Feng, 2013).

With a relationship established between $\delta^{18}\text{O}_{\text{diatom}}$ and regional Central Asian precipitation around Lake Baikal, records of precipitation from the lake have the potential to aid the development of future forecasts for the region. Models in the Coupled Model Intercomparison Project (CMIP5) are currently not able to confidently predict future changes in Central Asian precipitation (Christensen et al., 2013), but together with regional models they indicate the potential for decreases in precipitation for northern Mongolia and the Lake Baikal catchment, leading to associated reductions in soil moisture and increased vulnerability to drought and fire (Sato et al., 2007; Törnqvist et al., 2014). Data-model comparisons under the Paleoclimate Modelling Intercomparison Project (PMIP) highlight the complexities in generating accurate simulation of precipitation for the mid-Holocene (Bartlein et al., 2010; Braconnot et al., 2012). Whereas PMIP3 simulations suggest that regional conditions were drier in the mid-Holocene compared to pre-industrial conditions (Bartlein et al., 2017), our low-resolution results suggest that regional precipitation at 6 ka was c. 25% higher than modern (450 mm/yr) and c. 30% higher than reconstructed precipitation of 430 mm/yr in pre-industrial conditions at c. 1850 AD (Fig. 7). Further investigations on the controls of $\delta^{18}\text{O}_{\text{diatom}}$ in Lake Baikal, in an attempt to better constraint the divergence with pollen reconstructed precipitation through the mid/late Holocene, together with higher resolution measurements through the Holocene and integration of these results within ongoing modelling efforts therefore holds the potential to aid future model validations for Central Asia. In particular, higher resolution records will provide greater insight into the abrupt changes in precipitation that are superimposed on the Holocene record from Vydrino Shoulder, events that may be concordant with ice-rafted debris events in the North Atlantic Ocean (Mackay et al., 2011).

5 Conclusions

There is uncertainty over the potential for future changes in Central Asian precipitation under a warmer climate state, changes which have severe implications for the grassland-taiga ecotone and carbon cycling in the region. By comparing records of $\delta^{18}\text{O}_{\text{diatom}}$ to local meteorological data for the last 100 years we demonstrate an empirical relationship in Lake Baikal between $\delta^{18}\text{O}_{\text{diatom}}$ and Central Asian precipitation, providing an opportunity to study the long-term variability of regional precipitation. Accordingly, $\delta^{18}\text{O}_{\text{diatom}}$ records from Lake Baikal have the potential to aid future climate predictions by investigating geological intervals that might represent an analogue of a future climate state and through data-model comparisons. Results here from Holocene measurements of $\delta^{18}\text{O}_{\text{diatom}}$ show that precipitation has varied significantly over the last 10 ka, indicating the region's potential sensitivity to a perturbation in the climate system, with levels of precipitation

over the past c. 160 years either at or close to their lowest levels of the last 10 ka.

References

- Afanasyev, A.N., 1976. The Water Resources and Water Balance of Lake Baikal Basin. Nauka Publishers, Novosibirsk. (in Russian).
- Appleby, P.G., Oldfield, F., 1978. The calculation of ^{210}Pb dates assuming a constant rate of supply of unsupported ^{210}Pb to the sediment. *Catena* 5, 1-8.
- Appleby, P.G., Nolan, P.J., Gifford, D.W., Godfrey, M.J., Oldfield, F., Anderson, N.J., Battarbee, R.W., 1986. ^{210}Pb dating by low background gamma counting. *Hydrobiologia* 141, 21-27.
- Appleby, P.G., Richardson, N., Nolan, P.J., 1992. Self-absorption corrections for well-type germanium detectors. *Nucl. Instrum. Meth. B* 71, 228-233.
- Bartington Instruments 1995. Operation Manual MS2. Bartington Instruments, Oxford, <http://www.bartington.com/Literaturepdf/Operation%20Manuals/om0408%20MS2.pdf>.
- Bartlein, P.J., Harrison, S.P., Brewer, S., Connor, S., Davis, B.A.S., Gajewski, K., Guiot, J., Harrison-Prentice, T.I., Henderson, A., Peyron, O., Prentice, I.C., Scholze, M., Seppä, H., Shuman, B., Sugita S., Thompson, R.S., Vial, A.E., Williams, J., Wu, H., 2010. Pollen-based continental climate reconstructions at 6 and 21 ka: a global synthesis. *Clim. Dyn.* 3-4, 775-802.
- Bartlein, P.J., Harrison, S.P., Izumi, K., 2017., Underlying causes of Eurasian midcontinental aridity in simulations of mid-Holocene climate, *Geophys. Res. Lett.* 44, 9020-9028.
- Battarbee, R.W., Mackay, A.W., Jewson, D., Ryves, D.B., Sturm, M., 2005., Differential dissolution of Lake Baikal diatoms: correction factors and implications for palaeoclimatic reconstruction. *Global Planet Change.* 46,75-86.
- Braconnot, P., Harrison, S.P., Kageyama, M., Bartlein, P.J., Masson-Delmotte, V., Abe-Ouchi, A., Otto-Bliesner, B., Zhao, Y., 2012., Evaluation of climate models using palaeoclimatic data. *Nat. Clim. Change* 2, 417-424.
- Brewer, T., Leng, M., Mackay, A.W., Lamb, A., Tyler, J., Marsh, N., 2008. Unravelling contamination signals in biogenic silica oxygen isotope composition: the role of major and trace element geochemistry. *J Quaternary Sci.* 23, 365-374.
- Bush, A.B.G., 2005. $\text{CO}_2/\text{H}_2\text{O}$ and orbitally driven climate variability over central Asia through the Holocene. *Quatern. Int.* 136, 15-23.
- Chapligin, B., Leng, M.J., Webb, E., Alexandre, A., Dodd, J.P., Ijiri, A., Lücke, A., Shemesh, A., Abelmann, A., Herzsuh, U., Longstaffe, F.J., Meyer, H., Moschen, R., Okazaki, Y., Rees, N., Sharp, Z.D., Sloane, H.J., Sonzogni, C., Swann, G.E.A., Sylvestre, F., Tyler, J.T., Yam, R., 2011. Inter-laboratory comparison of oxygen isotopes from biogenic silica. *Geochim. Cosmochim. Ac.* 75, 7242-7256.
- Chen, S-J., Kuo, Y-H., Zhang, P-Z., Bai, Q-F., 1991. Synoptic climatology of cyclogenesis over East Asia. *Mon. Weather Rev.* 119, 1407-1418.
- Christensen, J.H., Krishna Kumar, K., Aldrian, E., An, S.-I., Cavalcanti, I.F.A., de Castro, M., Dong, W., Goswami, P., Hall, A., Kanyanga, J.K., Kitoh, A., Kossin, J., Lau, N.-C., Renwick, J., Stephenson, D.B., Xie, S.-P., Zhou, T., 2013. Climate Phenomena and their Relevance for Future Regional Climate Change. In: *Climate Change 2013: The Physical Science Basis. Contribution of Working Group I to the Fifth Assessment Report of the Intergovernmental Panel on Climate Change* [Stocker, T.F., Qin, D., Plattner, G.-K., Tignor, M., Allen, S.K., Boschung, J., Nauels, A., Xia, Y., Bex, V. Midgley, P.M. (eds.)]. Cambridge University Press, Cambridge, United Kingdom and New York, NY, USA.
- Craine, J.M., Nippert, J.B., Elmore, A.J., Skibbe, A.M., Hutchinson, S.L., Brunsell, N.A., 2012, Timing of climate variability and grassland productivity. 109, *P. Natl. Acad. Sci. USA.* 3401-3405.
- Crowther, T.W., Todd-Brown, K.E.O., Rowe, C.W., Wieder, W.R., Carey, J. C., Machmuller, M.B., Snoek, B.L., Fang, S., Zhou, G., Allison, S.D., Blair, J.M., Bridgham, S.D., Burton, A.J., Carrillo, Y., Reich, P.B., Clark, J.S., Classen, A.T., Dijkstra, F.A., Elberling, B., Emmett, B.A., Estiarte, M., Frey, S.D., Guo, J., Harte, J., Jiang, L., Johnson, B.R., Kröel-Dulay, G., Larsen, K.S., Laudon, H., Lavalley, J.M., Luo, Y., Lupascu, M., Ma, L.N., Marhan, S., Michelsen, A., Mohan, J., Niu, S., Pendall, E., Peñuelas, J., Pfeifer-Meister, L., Poll, C., Reinsch, S., Reynolds, L.L., Schmidt, I.K., Sistla, S., Sokol, N.W., Templer, P.H., Treseder, K.K., Welker, J.M., Bradford, M.A., 2016. Quantifying global soil carbon losses in response to warming. *Nature* 540, 104-108.
- Davi, N.K., Jacoby, G.C., Curtis, A.E., Nachin, B., 2006. Extension of drought records for central Asia using tree rings: West central Mongolia. *J. Clim.*, 19, 288-299.
- Davi, N., Jacoby, G., D'Arrigo, R., Baatarbileg, N., Li, J., Curtis, A., 2009. A tree-ring based drought index reconstruction for far western Mongolia: 1565–2004. *Int. J. Climatol.* 29, 1508-1514.

- 551 Davi, N., Jacoby, G., Fang, K., Li, J., D'Arrigo, R., Baatarbileg, N., Robinson, D., 2010. Reconstructing drought
552 variability for Mongolia based on a large-scale tree ring network: 1520-1993. *J. Geophys. Res.* 115, D22103.
- 553 Endo, N., Kadota, T., Matsumoto, J., Ailikun, B., Yasunari, T., 2006. Climatology and Trends in Summer Precipitation
554 Characteristics in Mongolia for the Period 1960–98. *J. Meteorol. Soc. Jpn.* 84, 543-551.
- 555 Frolova, N.L., Belyakova, P.A., Grigoriev, V.Y., Sazonov, A.A., Zotov, L.V., Jarsjö, J., 2017. Runoff fluctuations in the
556 Selenga River Basin. *Reg. Environ. Change*. doi:10.1007/s10113-017-1199-0.
- 557 Forkel, M., Thonicke, K., Beer, C., Cramer, W., Bartalev, S., Schmullius, C., 2012. Extreme fire events are related to
558 previous-year surface moisture conditions in permafrost-underlain larch forests of Siberia. *Environ. Res. Lett.* 7,
559 044021.
- 560 Hansen, M.C., Potapov, P.V., Moore, R., Hancher, M., Turubanova, S.A., Tyukavina, A., Thau, D., Stehman, S.V., Goetz,
561 S.J., Loveland, T.R., Kommareddy, A., Egorov, A., Chini, L., Justice, C.O., Townshend, J.R.G., 2013. High-resolution
562 global maps of 21st-century forest cover change. *Science* 342, 850-853.
- 563 Haywood, A.M., Dowsett, H.J., Dolan, A.M., 2016. Integrating geological archives and climate models for the mid-
564 Pliocene warm period. *Nat. Commun.* 7, 10646.
- 565 Hijioka, Y., Lin, E., Pereira, J.J., Corlett, R.T., Cui, X., Insarov, G.E., Lasco, R.D., Lindgren, E., Surjan, A., 2014. Asia, in:
566 Barros, V.R., Field, C.B., Dokken, D.J., Mastrandrea, M.D., Mach, K.J., Bilir, T.E., Chatterjee, M., Ebi, K.L., Estrada,
567 Y.O., Genova, R.C., Girma, B., Kissel, E.S., Levy, A.N., MacCracken, S., Mastrandrea, P.R., White, L.L. (Eds.),
568 Climate Change 2014: Impacts, Adaptation, and Vulnerability. Part B: Regional Aspects. Contribution of Working
569 Group II to the Fifth Assessment Report of the Intergovernmental Panel on Climate Change. Cambridge University
570 Press, Cambridge, United Kingdom and New York, NY, USA, pp. 1327-1370.
- 571 Hohmann R., Kipfer R., Peeters F., Piepke G., Imboden D.M., Shimaraev M.N., 1997. Deep-water renewal in Lake Baikal.
572 *Limnol. Oceanogr.* 42, 841-855.
- 573 IPCC, 2012. Managing the Risks of Extreme Events and Disasters to Advance Climate Change Adaptation. A Special
574 Report of Working Groups I and II of the Intergovernmental Panel on Climate Change, in: Field, C.B., Barros, V.,
575 Stocker, T.F., Qin, D., Dokken, D.J., Ebi, K.L., Mastrandrea, M.D., Mach, K.J., Plattner, G.-K., Allen, S.K., Tignor, M.,
576 Midgley, P.M. (Eds.), Cambridge University Press, Cambridge, UK, and New York, NY, USA, 582 pp.
- 577 Iwao, K., Ttakahashi, M., 2006. Interannual change in summertime precipitation over northeast Asia. *Geophys. Res. Lett.*
578 33, L16703.
- 579 Iwao, K., Ttakahashi, M., 2008. A Precipitation seesaw mode between Northeast Asia and Siberia in Summer caused by
580 Rossby waves over the Eurasian continent. *J. Clim.* 21, 2401-2419.
- 581 Karthe, D., Chalov, S., Borchardt, D., 2015. Water resources and their management in central Asia in the early twenty first
582 century: status, challenges and future prospects. *Environ. Earth. Sci.* 73, 487-499.
- 583 Kavvada, A., Ruiz-Barradas, A., Nigam, S., 2013, AMO's structure and climate footprint in observations and IPCC AR5
584 climate simulations. *Clim. Dyn.* 41, 1345-1364.
- 585 Kipfer, R., Aeschbach-Hertig, W., Hofer, M., Hohmann, R., Imboden, D.M., Baur, H., Golubev, V., Klerkx, J., 1996.
586 Bottomwater formation due to hydrothermal activity in Frolikha Bay, Lake Baikal, eastern Siberia. *Geochim.*
587 *Cosmochim. Acta.* 60, 961-971.
- 588 Kostrova, S.S., Meyer, H., Chaplign, B., Kossler, A., Bezrukova, E.V., Tarasov, P.E., 2013., Holocene oxygen isotope
589 record of diatoms from Lake Kotokel (southern Siberia, Russia) and its palaeoclimatic implications. *Quatern Int.* 290-
590 291, 21-34.
- 591 Kurita, N., Yoshida N., Inoue, G., Chayanova, E.A, 2004., Modern isotope climatology of Russia: A first assessment. *J*
592 *Geophys Res.* 109, D03102, doi:10.1029/2003JD003404.
- 593 Leng, M.J., Barker, P., 2006. A review of the oxygen isotope composition of lacustrine diatom silica for palaeoclimate
594 reconstruction. *Earth Sci. Rev.* 75, 5-27.
- 595 Leng, M.J., Sloane, H.J., 2008. Combined oxygen and silicon isotope analysis of biogenic silica. *Journal of Quaternary*
596 *Science* 23, 313-319.
- 597 Li, C., Zhang, C., Luo, G., Chen, X., Maisupova, B., Madaminov, A.A., Han, Q., Djenbaev, B.M., 2015. Carbon stock and
598 its responses to climate change in Central Asia. *Glob. Change. Biol.* 21, 1951-1967.
- 599 Liu, Y.Y., Evans, J.P., McCabe, M.F., de Jeu, R.A.M., van Dijk, A.I.J.M., Dolman, A.J., Saizen, I., 2013. Changing Climate
600 and Overgrazing Are Decimating Mongolian Steppes. *PLOS One* 8, e57599.
- 601 Lu, Y., Zhuang, Q., Zhou, G., Sirin, A., Melillo, J., Kicklighter, D., 2009. Possible decline of the carbon sink in the
602 Mongolian Plateau during the 21st century. *Environ. Res. Lett.* 4, 045023.
- 603 Lydolph, P.E., 1977. Eastern Siberia. In: *Climates of the Soviet Union. World Survey of Climatology*, vol. 7. Elsevier, pp.
604 91-115.

- 605 Mackay, A., Flower, R., Kuzmina, A., Granina, L., Rose, N., Appleby, P., Boyle, J., and Battarbee, R., 1998., Diatom
606 succession trends in recent sediments from Lake Baikal and their relation to atmospheric pollution and to climate
607 change, *Philos. T. Roy. Soc. B*, 353, 1011-1055.
- 608 Mackay, A.W., Karabanov, E., Khursevich, G., Leng, M., Morley, D.W., Panizzo, V.N., Sloane, H.J., Williams, D., 2008.
609 Reconstructing hydrological variability in Lake Baikal during MIS 11: an application of oxygen isotope analysis of
610 diatom silica. *J Quaternary Sci.*, 23, 365-374.
- 611 Mackay, A.W., Swann, G.E.A., Brewer, T., Leng, M.J., Morley, D.W., Piotrowska, N., Rioual, P., White, D., 2011. A
612 reassessment of late glacial-Holocene diatom oxygen isotope records from Lake Baikal using a mass balance approach.
613 *J Quaternary Sci.* 26, 627-634
- 614 Mackay, A.W., Swann, G.E.A., Fagel, N., Fietz, S., Leng, M.J., Morley, D., Rioual, P., Tarasov, P. 2013., Hydrological
615 instability during the Last Interglacial in central Asia: a new diatom oxygen isotope record from Lake Baikal.
616 *Quaternary Sci. Rev.* 66, 45-54.
- 617 Mackay, A.W., Seddon, A.W.R., Leng, M.J., Heumann, G., Morley, D.W., Piotrowska, N., Rioual, P., Roberts, S., Swann,
618 G.E.A., 2017. Holocene carbon dynamics at the forest - steppe ecotone of southern Siberia. *Glob. Change Biol.* 23,
619 1942-1960.
- 620 Moore, G.W.K., Halfar, J., Majeed, H., Adey, W., Kronz, A., 2017, Amplification of the Atlantic Multidecadal Oscillation
621 associated with the onset of the industrial-era warming. *Sci Rep-UK*, 7:40861.
- 622 Moore, M.V., Hampton, S.E., Izmet'eva, L.R., Silow, E.A., Peshkova, E.V., Pavlov, B.K., 2009. Climate Change and the
623 World's "Sacred Sea"-Lake Baikal, Siberia. *BioScience* 49, 405-417.
- 624 Morley, D.W., Leng, M.J., Mackay, A.W., Sloane, H.J., 2005. Late Glacial and Holocene atmospheric circulation change in
625 the Lake Baikal region documented by oxygen isotopes from diatom biogenic silica. *Global Planet. Change* 46, 221-
626 233.
- 627 PAGES Hydro2k Consortium, 2017., Comparing proxy and model estimates of hydroclimate variability and change over
628 the Common Era, *Clim Past*, 13, 1851-1900,
- 629 Panizzo V.N., Swann, G.E.A., Mackay, A.W., Vologina, E., Alleman, L., Andre, L., Pashley, V.H., Horstwood, M.S.A.,
630 2017., Constraining modern day silicon cycling in Lake Baikal. *Global Biogeochem Cy.* 31, 556-574.
- 631 Pederson, N., Jacoby, G., D'Arrigo, R., Cook, E., Buckley, B., Dugarjav, C., Mijiddorj, R., 2001. Hydrometeorological
632 reconstructions for north-eastern Mongolia derived from tree rings: AD 1651–1995, *J. Clim.* 14, 872-881.
- 633 Popovskaya, G.I., 2000. Ecological monitoring of phytoplankton in Lake Baikal. *Aquatic Ecosystem Health and*
634 *Management* 3, 215-225.
- 635 Randerson, J.T., Liu, H., Flanner, M.G., Chambers, S.D., Jin, Y., Hess, P.G., Pfister, G., Mack, M.C., Treseder, K.K.,
636 Welp, L.R., Chapin, F.S., Harden, J.W., Goulden, M.L., Lyons, E., Neff, J.C., Schuur, E.A.G., Zender, C.S., 2006.
637 The Impact of Boreal Forest Fire on Climate Warming. *Science* 314, 1130-1132.
- 638 Ravens, T.M., Kocsis, O., Wüest, A., Granin, N., 2000. Small-scale turbulence and vertical mixing in Lake Baikal. *Limnol.*
639 *Oceanogr.* 45, 159-173.
- 640 Rioual, P., Mackay, A.W., 2005., A diatom record of centennial resolution for the the Kazantsevo Interglacial stage in Lake
641 Baikal (Siberia). *Global Planet Change* 46, 199-219.
- 642 Romanovsky, V.E., Drozdov, D.S., Oberman, N.G., Malkova, G.V., Kholodov, A.L., Marchenko, S.S., Moskalenko, N.G.,
643 Sergeev, D.O., Ukraintseva, N.G., Abramov, A.A., Gilichinsky, D.A., Vasiliev, A.A., 2010., Thermal state of permafrost
644 in Russia. *Permafrost Periglac.* 21, 136-155.
- 645 Ryves, D.B., Jewson, D.H., Sturm, M., Battarbee, R.W., Flower, R.J., Mackay, A.W., Granin, N. G., 2003., Quantitative
646 and qualitative relationships between planktonic diatom communities and diatom assemblages in sedimenting material
647 and surface sediments in Lake Baikal, Siberia. *Limnol. Oceanogr.*, 48, 1643–1661.
- 648 Sato, T., Kimura, F., Kitoh, A., 2007. Projection of global warming onto regional precipitation over Mongolia using a
649 regional climate model. *J. Hydrol.* 333, 144-154.
- 650 Schuur, E.A.G., McGuire, A.D., Schädel, C., Grosse, G., Harden, J.W., Hayes, D.J., Hugelius, G., Koven, C.D., Kuhry, P.,
651 Lawrence, D.M., Lawrence, S.M., Olefeldt, D., Romanovsky, V.E., Schaefer, K., Turetsky, M.R., Treat, C.C., Vonk,
652 J.E., 2015. Climate change and the permafrost carbon feedback. *Nature* 520, 171-179.
- 653 Seal, R.R., Shanks, W.C., 1998. Oxygen and hydrogen isotope systematics of Lake Baikal, Siberia: implications for
654 palaeoclimate studies. *Limnol. Oceanogr.* 43, 1251-1261.
- 655 Selvam, B.P., Lapierre, J-F., Guillemette, F., Voigt, C., Lamprecht, R.E., Biasi, C., Christensen, T.R., Martikainen, P.J.,
656 Berggren, M., 2017. Degradation potentials of dissolved organic carbon (DOC) from thawed permafrost peat. *Sci Rep-*
657 *UK* 7, 45811.
- 658 Seim, A., Schultz, J., Leland, C., Davi, N., Byambasuren, O., Liang, E., Wang, X., Beck, C., Linderholm, H.W., Pederson,

- 659 N., 2017., Synoptic-scale circulation patterns during summer derived from tree rings in mid-latitude Asia. *Clim Dyn.*
660 49, 1917-1931.
- 661 Settele, J., Scholes, R., Betts, R., Bunn, S., Leadley, P., Nepstad, D., Overpeck, J.T., Taboada, M.A., 2014, Terrestrial and
662 inland water systems, in Field, C.B., Barros, V.R., Dokken, D.J., Mach, K.J., Mastrandrea, M.D., Bilir, T.E., Chatterjee,
663 M., Ebi K.L., Estrada, Y.O., Genova, R.C., Girma, B., Kissel, E.S., Levy, A.N., MacCracken, S., Mastrandrea, P.R.,
664 White, L.L. (Eds.), *Climate Change 2014: Impacts, Adaptation, and Vulnerability. Part A: Global and Sectoral Aspects.*
665 *Contribution of Working Group II to the Fifth Assessment Report of the Intergovernmental Panel on Climate Change.*
666 Cambridge University Press, Cambridge, United Kingdom and New York, NY, USA, pp. 271-359.
- 667 Shahgedanova, M., 2002. Climate at present and in the historical past. In: Shahgedanova, M. (Ed.), *The Physical*
668 *Geography of Northern Eurasia.* OUP, Oxford, pp. 70-102.
- 669 Sharkuu N., 1998. Trends in permafrost development in the Selenge River basin, Mongolia. *Collection Nordicana*, 55,
670 979-985.
- 671 Shimaraev M.N., Granin N.G., 1991. Temperature stratification and the mechanisms of convection in Lake Baikal. *Dokl.*
672 *Akad. Nauk.* 321, 381-385.
- 673 Shimaraev M.N., Domysheva V.M., 2004. Climate and long-term silica dynamics in Lake Baikal. *Russ. Geol. Geophys.*
674 45, 310-316.
- 675 Shimaraev M.N., Granin N.G., Zhdanov A.A., 1993. Deep ventilation of Lake Baikal waters due to spring thermal bars.
676 *Limnol. Oceanogr.* 38, 1068-1072.
- 677 Shimaraev, M.N., Verbolov, V.I., Granin, N.G., Sherstyankin, P.P., 1994. Physical Limnology of Lake Baikal. A review. In:
678 Shimaraev, M.N., Okuda, S. (Eds.), *BICER Publishers, Irkutsk.* 81 pp.
- 679 Shimaraev, M.N., Troitskaya, E.S., Blinov, V.V., Ivanov, V.G., Gnatovskii, R.Yu., 2012. Upwellings in Lake Baikal. *Dokl.*
680 *Earth Sc.* 442, 272-276.
- 681 Solovieva, N., Tarasov P.E., MacDonald, G., 2005. Quantitative reconstruction of Holocene climate from the Chuna Lake
682 pollen record, Kola Peninsula, northwest Russia. *Holocene* 15, 141-148.
- 683 Sturm M., Vologina E.G., Vorob'eva S.S., 2016. Holocene and Late Glacial sedimentation near steep slopes in southern
684 Lake Baikal. *J. Limnology.* 75, 24-35.
- 685 Sugita, M., Yoshizawa, S., Byambakhuu, I., 2015, Limiting factors for nomadic pastoralism in Mongolian steppe: a
686 hydrologic perspective. *J. Hydrol.* 524, 455-467.
- 687 Sun, C., Li, J., Zhao, S., 2015. Remote influence of Atlantic multidecadal variability on Siberian warm season
688 precipitation. *Sci. Rep-UK.* 5, 16853.
- 689 Swann, G.E.A., Pike, J., Snelling, A.M., Leng, M.J., Williams, M.C., 2013. Seasonally resolved diatom $\delta^{18}\text{O}$ records from
690 the west Antarctic Peninsula over the last deglaciation. *Earth Planet. Sci. Lett.* 364, 12-23.
- 691 Tarasov, P., Bezrukova, E., Karabanov, E., Nakagawa, T., Wagner, M., Kulagina, N., Letunova, P., Abzaeva, A.,
692 Granoszewski, W., Riedel, F., 2007. Vegetation and climate dynamics during the Holocene and Eemian interglacials
693 derived from Lake Baikal pollen records. *Palaeogeogr. Palaeoclimatol.* 252, 440-457.
- 694 Tarasov, P.E., Bezrukova, E.V., Krivonogov, S.K., 2009. Late Glacial and Holocene changes in vegetation cover and
695 climate in southern Siberia derived from a 15 kyr long pollen record from Lake Kotokel. *Clim. Past.* 5, 285-295.
- 696 Tautenhahn, S.T., Lichstein, J.W., Jung, M., Kattge, J., Bohlman, S.A., Heilmeyer, H., Prokushkin, A., Kahl, A., Wirth, C.,
697 2016. Dispersal limitation drives successional pathways in Central Siberian forests under current and intensified fire
698 regimes. *Glob. Change Biol.* 22, 2178-2197.
- 699 Tchebakova, N.M., Parfenova, E., Soja, A.J., 2009. The effects of climate, permafrost and fire on vegetation change in
700 Siberia in a changing climate. *Environ. Res. Lett.* 4 045013.
- 701 Tchebakova, N.M., Parfenova, E.I., Korets, M.A., Conard, S.G., 2016. Potential change in forest types and stand heights in
702 central Siberia in a warming climate. *Environ. Res. Lett.* 11, 035016.
- 703 Törnqvist, R., Jarsjö, J., Pietroni, J., Bring, A., Rogberg, P., Asokan, S.M., Destouni, G., 2014. Evolution of the hydro-
704 climate system in the Lake Baikal basin. *J. Hydrol.* 519, 1953-1962.
- 705 Troitskaya, E., Blinov, V., Ivanov, V., Zhdanov, A., Gnatovsky, R., Sutyryna, E., Shimaraev, M., 2015. Cyclonic circulation
706 and upwelling in Lake Baikal. *Aquat. Sci.* 77, 171-182.
- 707 Tsimitri, C., Rockel, B., Wüest, A., Budnev, N.M., Sturm, M., Schmid, M., 2015. Drivers of deep-water renewal events
708 observed over 13 years in the South Basin of Lake Baikal. *J. Geophys. Res. Oceans*, 120, 1508-1526.
- 709 Vologina, E.G., Kashik, S.A., Sturm, M., Vorob'eva, S.S., Lomonosova, T.K., Kalashnikova, I.A., Khramtsova, T.I.,
710 Toshchakov, S.Yu., 2007. Results of research into Holocene sediments of the South and Central basins of Lake Baikal
711 (BDP-97 and short cores). *Russ. Geol. Geophys.* 48, 312-323.

- 712 Weiss, R.F., Carmak, E.C., Koropalov, V.M., 1991. Deep-water renewal and biological production in Lake Baikal. *Nature*
713 349, 665-669.
- 714 Wang, W., Feng, Z., 2013. Holocene moisture evolution across the Mongolian Plateau and its surrounding areas: A
715 synthesis of climatic records. *Earth-Sci. Rev.* 122, 38-57.
- 716 Wu, X, Liu, H, Guo, D, Anenkhonov, O.A., Badmaeva, N.K., Sanddanov, D.V., 2012. Growth Decline Linked to Warming-
717 Induced Water Limitation in Hemi-Boreal Forests. *PLoS ONE* 7, e42619. doi:10.1371/journal.pone.0042619.
- 718 Zhao, L., Wu, Q., Marchenko, S.S., Sharkuu, N., 2010. Thermal state of permafrost and active layer in central Asia during
719 the International Polar Year. *Permafrost Periglac.* 21, 198-207.

720

721 **Acknowledgements**

722 This work was supported by Natural Environment Research Council grants NE/J00829X/1, NE/J010227/1, and
723 NE/J007765/1). The authors are indebted to the assistance of Nikolaj M. Budnev (Irkutsk State University), the
724 captain and crew of the Geolog research boat together with Dmitry Gladkochub (IEC) in facilitating and
725 organizing all Russian fieldwork. A final thanks is owed to Neil Rose and Handong Yang who carried out the
726 ²¹⁰Pb dating at the UCL Environmental Radiometric Facility and to the anonymous reviewers as well as guest
727 editor (Oliver Heiri) who's comments significantly improved the manuscript.

728

729 **Supplementary Information**

730 Supplementary Table 1: Diatom oxygen isotope ($\delta^{18}\text{O}_{\text{diatom}}$) and reconstructed precipitation for south basin
731 sediment cores BAIK13-1C, BAIK13-4F and BAIK13-7A used in the composite $\delta^{18}\text{O}_{\text{diatom}}$ record.

732

733 Supplementary Table 2: Holocene $\delta^{18}\text{O}_{\text{diatom}}$ from Vydrino Shoulder (Lake Baikal) (Mackay et al., 2011) and
734 reconstructed precipitation.